JOURNAL OF MATERIALS SCIENCE 27 (1992) 6770–6776

Cyclic tensile creep behaviour of cellulose nitrate and evaluation of constitutive equations

T. NISHITANI, M. TSUJI, H. OGURA
Department of Applied Mechanics, Suzuka College of Technology, Suzuka, 510-02, Japan

The cyclic creep behaviour under axial tension was quantitatively investigated using non-linear viscoelastic cellulose nitrate heated at 65 °C. The instantaneous strains at the instants of loading and unloading for three creep cycles and the creep strain rates during the three creep cycles were found to be influenced by the cycle numbers. However, the effect of the cycle number on the loading process was quite different from that on the unloading process in the cyclic creep deformation. The evaluation of the creep constitutive equations for the loading and unloading processes at one loading cycle deduced in the previous papers is discussed for the cyclic creep deformation. The deduced creep equations give good agreement with the actual observations for the three creep cycles independent of the cycle numbers and of the creep stress levels.

1. Introduction

In previous papers [1, 2], the creep behaviour under various combinations of superimposed tensile and hydrostatic loading were investigated using non-linear viscoelastic cellulose nitrate for the loading and unloading, respectively. Ordinary creep investigations are concerned with the loading or unloading process at only one loading cycle [1–5]. The deformation behaviour under cyclic creep may be different from that under the one loading cycle. In particular, the effect of the cycle number on creep behaviour in the loading process may be different from that in the unloading process.

In this work, the cyclic creep behaviour under axial tension was quantitatively investigated using the same non-linear viscoelastic cellulose nitrate heated at 65 °C as used in the previous papers [1, 2] for three creep cycles with various creep stress levels. The instantaneous strains at the instants of loading and unloading for each creep cycle and the creep strain-rates during the loading and unloading processes are discussed for the three creep cycles. The evaluation of the creep constitutive equations for the loading and unloading processes deduced in the previous papers [1, 2] is discussed for the cyclic creep deformation. The deduced creep constitutive equations give good agreement with the actual observations for the three creep cycles, independent of the cycle numbers and of the creep levels.

2. Constitutive equations for cyclic creep

2.1. Loading process

The principle of deducing the creep constitutive equation for the loading process of cyclic creep is the same as that in the previous paper [1]. In the present paper, axial tensile stress, $\sigma_1(\sigma_2 = \sigma_3 = 0)$, is applied to a uniaxial specimen. When the principal stress difference is denoted by $\Delta\sigma = \sigma_1 - \sigma_2$, the creep strain rate for principal strains is proposed to be [1]

$$\Delta\dot{\varepsilon}_c = B(t + s)^{\alpha}\Delta\sigma\exp[(b/3^{1/2})\Delta\sigma] \quad (1)$$

where t and s denote current time and material constant time, $\Delta\sigma$ is the principal stress difference, and B, α and b are material constants. On the other hand, the instantaneous elastic–plastic strain for principal strains was expressed as [1]

$$\Delta\varepsilon_0 = \frac{\Delta\sigma}{2G}[1 + (\Delta\sigma/3^{1/2}k)^{2n}] \quad (2)$$

where G, k and n are material constants. When it is necessary to calculate the total creep strain, $\Delta\varepsilon_c$, the following procedure is adopted. Time is subdivided into small intervals, $0 \to t_1$, $t_1 \to t_2$, ..., $t_{m-1} \to t_m$, .., t, in which the magnitude $\Delta\dot{\varepsilon}_c$ may be considered to be approximately constant. For example, $\Delta\varepsilon_c(t_m)$ at arbitrary time t_m in the period $t_{m-1} \to t_m$ is approximated as [1]

$$\Delta\varepsilon_c(t_m) = \Delta\varepsilon_c(t_{m-1}) + \Delta\dot{\varepsilon}_c(t_{m-1})(t_m - t_{m-1}) \quad (3)$$

The original point of the second creep cycle corresponds to the final instant of the unloading process of the 1st cycle as shown in Fig. 1, and the original point of the second creep cycle is considered as $t = 0$. The original point of the third creep cycle is also considered as $t = 0$ as shown in Fig. 1. Hence, the constitutive Equations 1 and 2 may be appropriate to the loading processes of the second and third creep cycles.

The material constants in Equations 1 and 2 depend on the cycle numbers as shown in Section 5.

2.2. Unloading process

The unloading process for each cycle begins at the last instant $t = t_*$ of the loading process, as shown in Fig. 1, and is considered as a new loading process

0022–2461

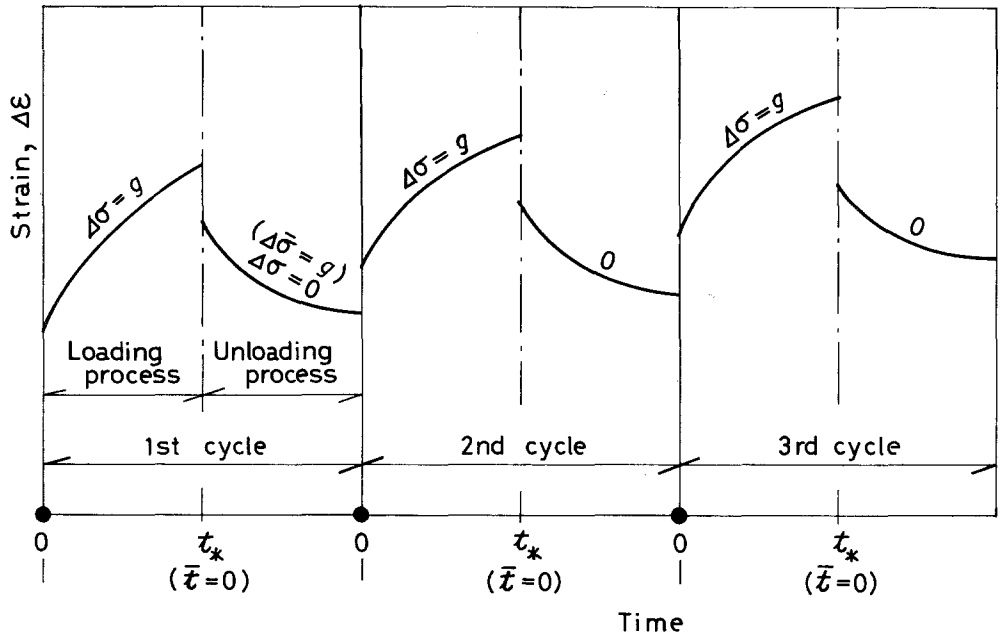

Figure 1 Schematic representation of creep relations for three creep cycles. (●) Original point of each creep cycle.

beginning at the instant $t = t_*$ [2]. The axes of the unloading process as shown in Fig. 1 of the previous paper [2] are directed in opposite directions to those of the preceding loading process. Parameters corresponding to the unloading co-ordinate are distinguished by the bar over the symbols [2]. In the non-linear viscoelastic deformation of the unloading process, as the instantaneous plastic strain is negligible, the strain, $\Delta\bar{\varepsilon}$, in the unloading process is proposed to consist of the three parts [2], namely, an instantaneous elastic part, $\Delta\bar{\varepsilon}_0$, a recovery creep part, $\Delta\bar{\varepsilon}_r$, and an additional creep part, $\Delta\bar{\varepsilon}_a$, as shown in Fig. 1 of the previous paper [2]. As the additional creep strain continues to appear in the early stage of the unloading process for the operating load, even in the unloading process, this deformation should also be taken into account [2]. The creep strain rate for principal strains in the unloading process was proposed by using the same concepts as used in the loading process [1, 2]

$$\begin{aligned}\Delta\dot{\bar{\varepsilon}}_c &= \Delta\dot{\bar{\varepsilon}}_r - \Delta\dot{\bar{\varepsilon}}_a \\ &= D(\bar{t} + s)^{\beta}\Delta\bar{\sigma}\exp[(d/3^{1/2})\Delta\bar{\sigma}] \\ &\quad - B'(t + s)^{\alpha}\Delta\sigma\exp[(b/3^{1/2})\Delta\sigma] \qquad (4)\end{aligned}$$

where the second term on the right-hand side corresponds to the additional creep strain-rate, $\Delta\dot{\bar{\varepsilon}}_a$. $\bar{t} = t - t_*$, $\Delta\bar{\sigma} = \Delta\sigma_* - \Delta\sigma$, and $\Delta\sigma_*$ corresponds to the value of $\Delta\sigma$ at time t_*. D, β, d, B' are material constants in the unloading process. However, when the load $\Delta\sigma$ is removed suddenly at the beginning of unloading process, as shown in Fig. 2 (namely, completely unloading creep), the additional creep strain rate, $\Delta\dot{\bar{\varepsilon}}_a$, becomes zero due to $\Delta\sigma = 0$ in the unloading process. The elastic strain in the unloading process for principal strains is expressed [2] as

$$\Delta\bar{\varepsilon}_0 = \Delta\bar{\sigma}/(2H) \qquad (5)$$

where H is a material constant. The total creep strain, $\Delta\bar{\varepsilon}_c$, is calculated by the same procedure as in Equation 3.

The unloading processes of the second and third creep cycles are considered as new loading processes beginning at the instant $t = t_*$ for their cycles as shown in Fig. 1. Hence, the constitutive Equations 4 and 5 may be appropriate to the unloading processes of the second and third creep cycles.

The material constants in Equations 4 and 5 depend on the cycle numbers as shown in Section 5.

3. Experimental procedure

The specimens used were the same as those used in the previous papers [1, 2], and were made of initially isotropic cellulose nitrate of thickness 6 mm. On the surface of each specimen, a square gauge mark was cut in a region of sufficiently uniform stress. The experimental apparatus used was the same as that in the previous papers [1, 2] and consisted of three major systems: a high-pressure generator and associated oil vessel with a heater; loading and unloading equipment with a load cell; and instruments to record the load and deformation. Detail descriptions of the apparatus and of the specimen are given by Ohashi [7], and a schematic drawing of the loading apparatus is given by Nishitani and Koike [8].

The creep tests were performed under axial tensile stress, σ_1 (hydrostatic pressure is equal to zero $\sigma_2 = \sigma_3 = 0$) for three creep cycles as shown in Fig. 2. Fig. 2 shows the creep stress–time diagrams for the three creep cycles with loading and unloading processes, where the time intervals $t = 0$–80 min and $t = 80$–160 min for each creep cycle correspond to the loading and unloading processes, respectively. Each stress was applied so as to obtain constant values of $\Delta\sigma = \Delta\bar{\sigma} = 6, 8, 10$ and 11.5 MPa for each creep cycle. When the stress, $\Delta\sigma = a$, is removed suddenly at the beginning of the unloading process which corresponds to $t = 80$ min or $\bar{t} = 0$ for each creep cycle in

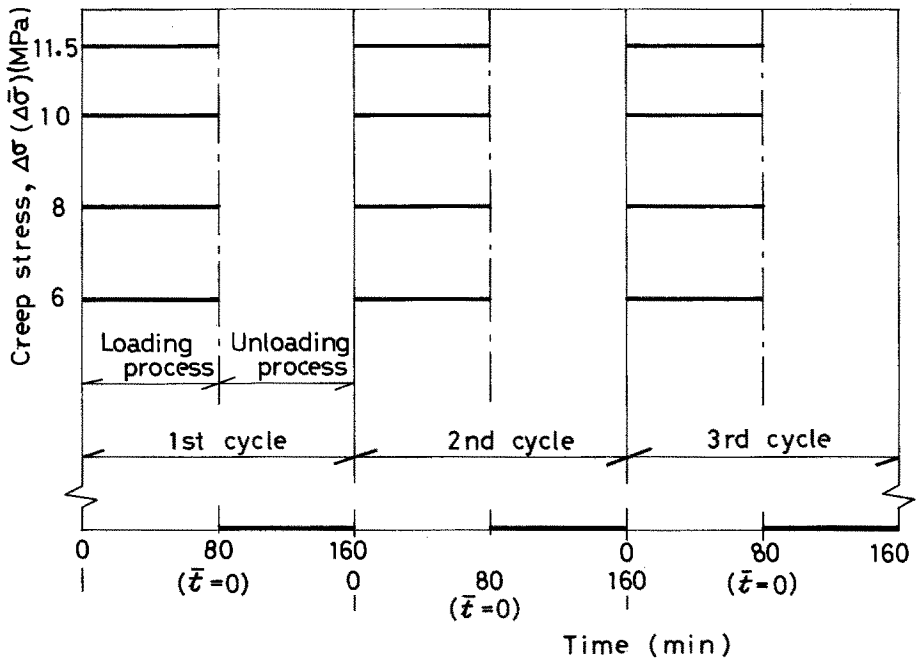

Figure 2 Creep stress–time diagrams for three creep cycles with loading and unloading processes.

Fig. 2, the condition $\Delta\sigma = 0$ corresponds to $\Delta\bar{\sigma} = a$ in the unloading process. In Fig. 2, time $t = 80$ min or $\bar{t} = 0$ for each creep cycle corresponds to the last instant of loading process, t_*, and corresponds to the original time of the unloading process. The original times of the second and third cycles are considered to have $t = 0$ as the new loading point, as shown in Fig. 2.

Axial elongation and cross contraction between gauge marks engraved on the specimen were measured to within 0.005 mm from photographs of the gauge marks using a magnifying projector. The accuracy of strain thus obtained is within about 2×10^{-4}. The principal strain difference $\Delta\varepsilon = \varepsilon_1 - \varepsilon_2$ was calculated in the natural strain system $\varepsilon_j = \ln(1 + e_j)$, where $e_j (j = 1, 2)$ are the conventional engineering strains.

4. Results

4.1. Loading process

The symbols in Fig. 3 show the experimental relations between the applied creep stress, $\Delta\sigma$, and the instantaneous elastic–plastic strain, $\Delta\varepsilon_0$, obtained from creep experiments at the instant of loading for each creep cycle at 65 °C, where it can be seen that a proportional dependence is not assumed for the first cycle, at least. Each symbol in Fig. 3 is plotted using the average of two tests. The elastic line is also shown. The value of $\Delta\varepsilon_0$ depends on the creep cycle number, and becomes smaller with increasing cycle number. The relation between $\Delta\sigma$ and $\Delta\varepsilon_0$ at the third cycle in Fig. 3 is almost equal to the elastic line, namely the instantaneous plastic strain tends to be zero at the third cycle.

Fig. 4 shows the experimental creep relations in the loading and unloading processes for the three creep cycles with various values of creep stresses. In Fig. 4, the loading process corresponds to time interval

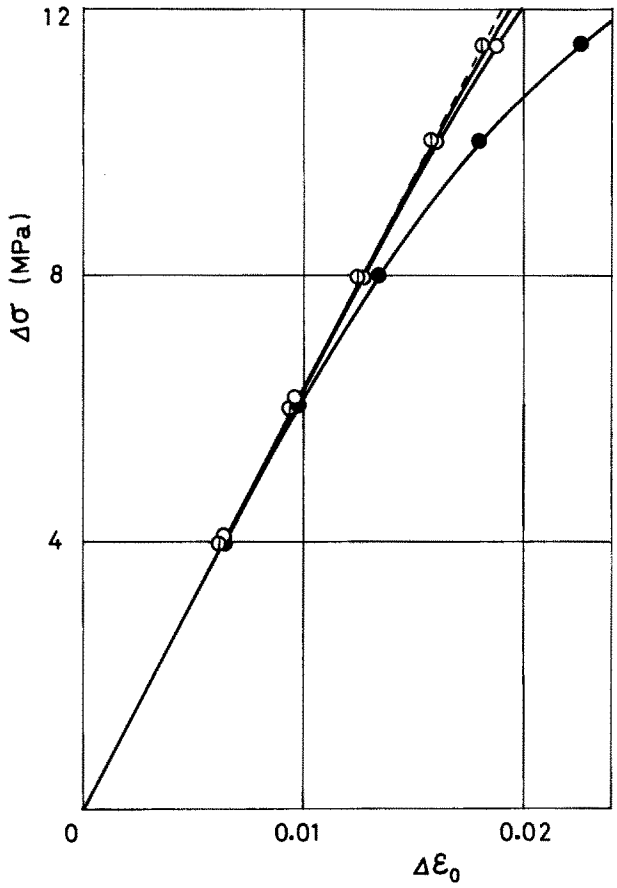

Figure 3 Relation between $\Delta\sigma$ and $\Delta\varepsilon_0$ at the instant of loading for each creep cycle. Cycle; (●) 1, (○) 2, (Φ) 3. (——) Equation 2, (---) the elastic line.

$t = 0$–80 min for each cycle. Each symbol in Fig. 4 is plotted using the average of two tests. In Fig. 4, the strain region over $\Delta\varepsilon = 0.28$ is supposed to be the microscopic crack zone in this paper. The solid curves in Fig. 5a and b show the relations between the creep strain-rate, $\Delta\dot{\varepsilon}_c$, and time with $\Delta\sigma = 11.5$ and 8 MPa in the loading process for each creep cycle, which

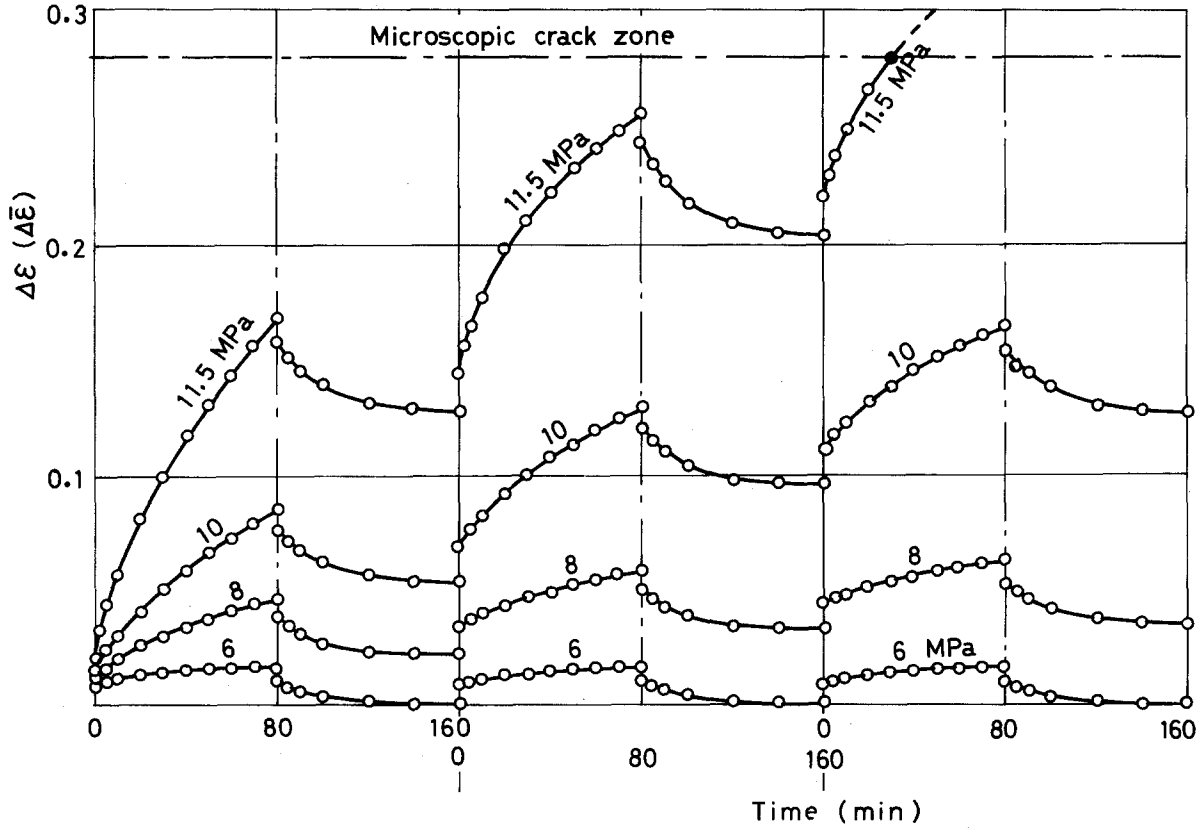

Figure 4 Experimental creep relations between $\Delta\varepsilon$ and $\Delta\bar{\varepsilon}$, and time in the loading and unloading processes for three creep cycles with each value of creep stress.

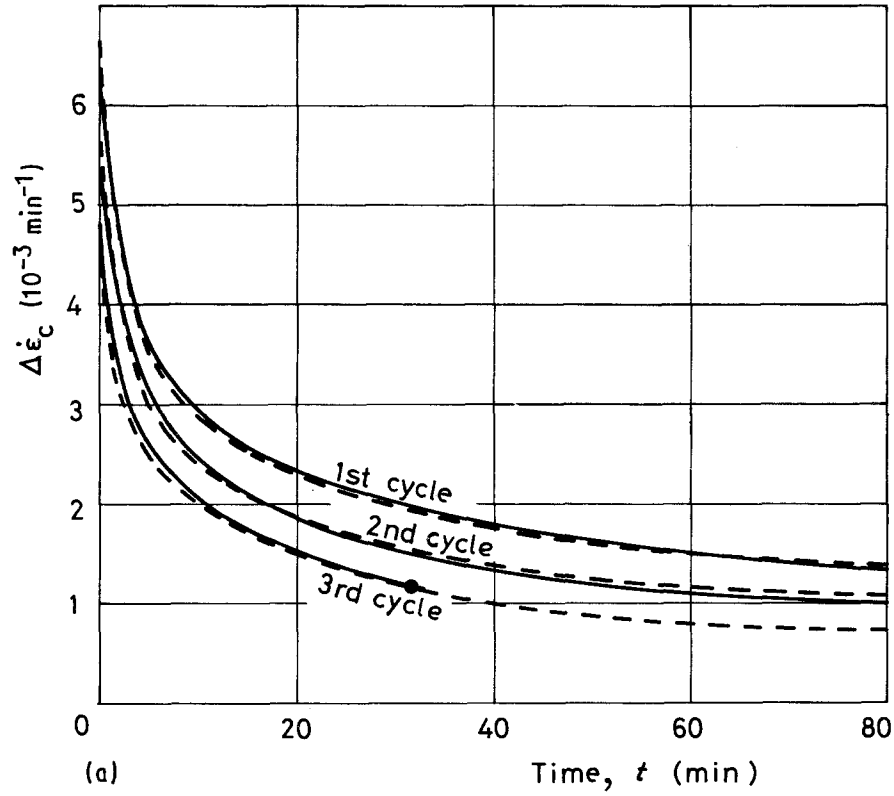

Figure 5 Relations between creep strain rate and time in the loading process for each creep cycle. (a) $\Delta\sigma$ = 11.5 MPa, (b) $\Delta\sigma$ = 8 MPa. (——) Experimental results, (– – –) Equation 1.

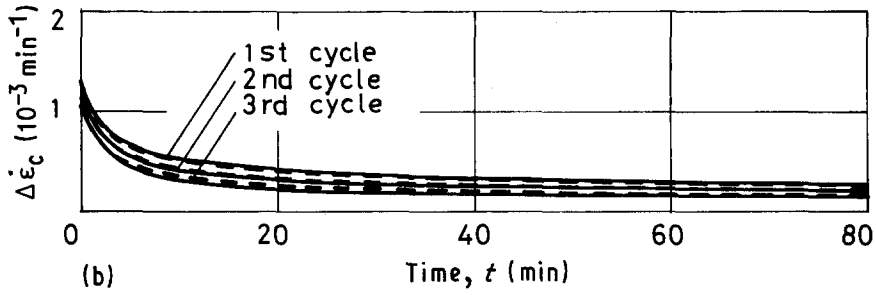

Figure 5 (continued)

correspond to the experimental results for the loading process shown in Fig. 4. The creep strain or the creep strain rate is strongly influenced by the cycle number, and the quality becomes smaller with increasing cycle number. Moreover, the trend is quite sensitive to the stress levels.

4.2. Unloading process

Fig. 6 shows the experimental relations between the applied creep stress, $\Delta\bar{\sigma}$, and the instantaneous elastic strain, $\Delta\bar{\varepsilon}_0$, obtained from the creep experiments at the instant of unloading for each creep cycle. The value of $\Delta\bar{\varepsilon}_0$ depends qualitatively on the creep cycle number, and tends to be larger with increasing cycle number. However, a proportional dependence in Fig. 6 may be approximately assumed for each cycle. The straight line through the original point of Fig. 5 is drawn using the method of least-square fit.

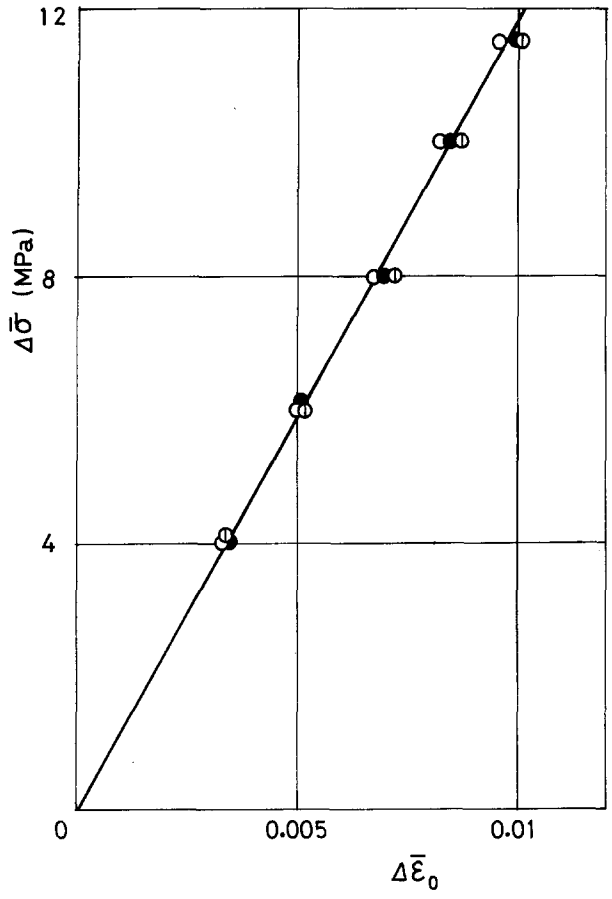

Figure 6 Relation between $\Delta\bar{\sigma}$ and $\Delta\bar{\varepsilon}_0$ at the instant of unloading for each creep cycle. Cycle: (●) 1, (○) 2, (Φ) 3.

The experimental creep relations in the unloading process are shown in Fig. 4, where the unloading process corresponds to time interval $t = 80$–160 min for each creep cycle. Fig. 7a and b show the relations between the creep strain rate, $\Delta\dot{\bar{\varepsilon}}_c$, and time in the unloading process for each creep cycle, which correspond to the experimental results for the unloading process shown in Fig. 4. Although the creep strain or the creep strain rate in the unloading process were influenced by the cycle number, their values become larger with increasing cycle number. This trend in the unloading process is reversed for the loading process.

5. Discussion

In Section 4, the creep behaviour was investigated in the loading and unloading processes under cyclic creep for various creep stress levels, and the effects of cyclic number on the instantaneous strain and creep strain rate were discussed. Here we discuss whether or not the deduced Equations 1, 2 for the loading process and Equations 4 and 5 for unloading process describe the actual observations independent of cycle numbers and of creep stress levels.

The material constants in Equations 1, 2 and 4, 5 can be determined experimentally. The procedure in the unloading process for each cycle is almost similar to that in the loading process for each cycle. Hence the procedure to determine the material constants in the loading process for the first cycle is shown in this paper, as an example. For creep test $\Delta\sigma = g$(const.) or $\Delta\dot{\sigma} = 0$,

$$\Delta\dot{\varepsilon}_c = B(t + s)^{\alpha}\exp[b(g/3^{1/2})](g) \qquad (6)$$

is obtained from Equation 1, and taking logarithms of both sides, the next form is obtained

$$\log(\Delta\dot{\varepsilon}_c/g) = \log B + \alpha\log(t + s) + 0.434\,b(g)/3^{1/2} \qquad (7)$$

As the values of $\Delta\dot{\varepsilon}_c$ and time t, are known from the experimental results, the values of B, α, s and b are approximately determined by the experiments at more than two different values of g.

The material constants in Equation 2 can be approximately determined from the experimental results between $\Delta\sigma$ and the instantaneous elastic–plastic strain, $\Delta\varepsilon_0$, at the instant of loading as shown in Fig. 3. As the relation $\Delta\varepsilon_0 = \Delta\sigma/(2G)$ is predominant while

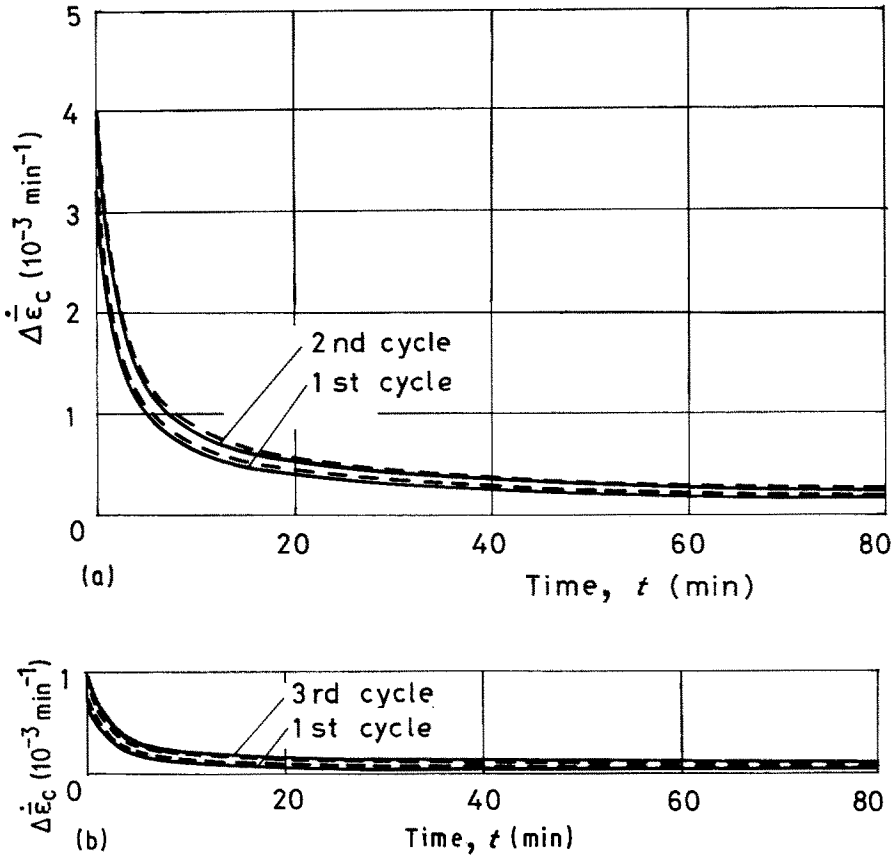

Figure 7 Relations between creep strain rate and time in the unloading process for each creep cycle. (a) $\Delta\bar{\sigma}$ = 11.5 MPa, (b) $\Delta\bar{\sigma}$ = 8 MPa. (——) Experimental results, (– – –) Equation 4.

the value of $\Delta\sigma$ is small, G can be easily determined. By denoting the known term in Equation 2 by A, we obtain

$$A = \Delta\varepsilon_0 - \frac{\Delta\sigma}{2G}$$

$$= \frac{1}{2G(3^{1/2}k)^{2n}}(\Delta\sigma)^{2n+1} \quad (8)$$

Taking logarithms of both sides, the above relation becomes

$$\log A = (2n + 1)\log\Delta\sigma - \log 2G(3^{1/2}k)^{2n} \quad (9)$$

Consequently, from the experimental result between $\Delta\sigma$ and the instantaneous elastic–plastic strain, $\Delta\varepsilon_0$, at the instant of loading, we can determine the values of n and k.

The material constants in Equations 1, 2 and 4, 5 determined by the procedures mentioned above are shown in Table I for the loading and unloading processes of the first creep cycle. The material constants except G, H and s were affected by the cycle number, as shown in Figs 8 and 9. The solid curves in Fig. 3 show the relations between $\Delta\sigma$ and $\Delta\varepsilon_0$ calculated from Equation 2 using the corresponding material constants shown in Table I and Fig. 8 for each cycle. The dashed curves in Fig. 5a and b show the relations between $\Delta\dot{\varepsilon}_c$ and time in the loading process calculated from Equation 1 using the corresponding material constants shown in Table I and Fig. 8 for each cycle. The dashed curves in Fig. 7a and b show the relations between $\Delta\dot{\bar{\varepsilon}}_c$ and time in the unloading process calculated from Equation 4 using the corresponding material constants shown in Table I and Fig. 9 for each cycle. These curves agree well with the corresponding experimental results expressed by the solid curves in Figs 5 and 7. The proposed relations in the loading and unloading processes for cyclic creep behaviour give good agreement with actual observations independent of the creep cycle number and of the creep stress level.

TABLE I Values of material constants for the first creep cycle

(a) Loading process

B (MPa^{-1} $min^{-(\alpha+1)}$)	s (min)	α	b (MPa^{-1})	G (MPa)	k (MPa)	n
7.7×10^{-6}	1.0	−0.35	0.65	315	9.2	1.85

(b) Unloading process

D (MPa^{-1} $min^{-(\beta+1)}$)	β	d (MPa^{-1})	B' ($MPa^{-1}min^{-(\alpha+1)}$)	H (MPa)
6.4×10^{-6}	−0.66	0.58	(9.4×10^{-7})	565

6. Conclusion

1. The instantaneous strains at the instants of loading and unloading for cyclic creep tests using nonlinear viscoelastic celluloid nitrate are influenced by

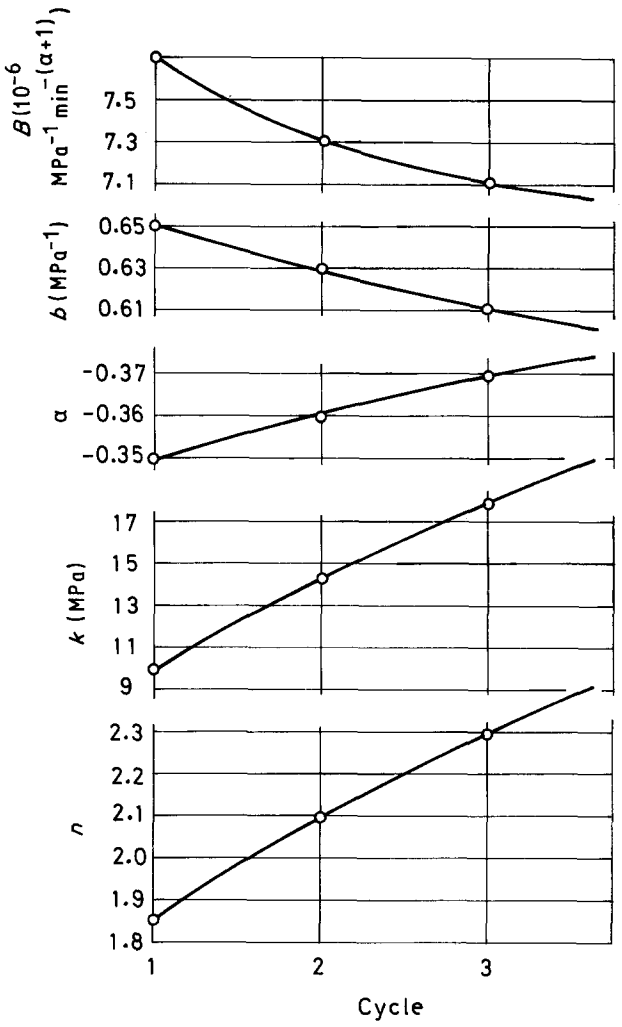

Figure 8 Relations between the material constants and creep cycle in the loading process.

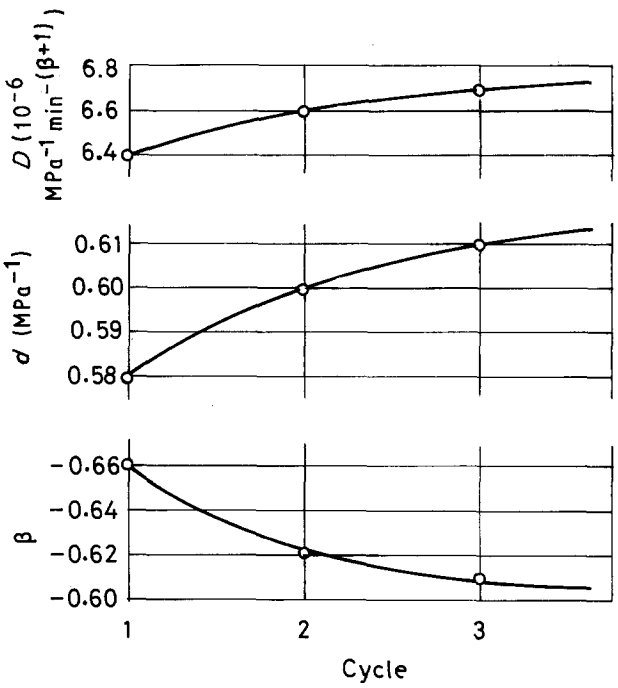

Figure 9 Relations between the material constants and creep cycle in the unloading process.

creep cycle number. The strain in the loading process decreases with increasing cycle number. However, the strain in the unloading process has a tendency to increase with increasing cycle number.

2. The creep strains in the loading and unloading processes for non-linear viscoelastic cellulose nitrate are remarkably influenced by creep cycle number. Although the creep strain in the loading process becomes smaller with increasing cycle number, that in the unloading process becomes larger with increasing cycle number. Moreover, those features affected by the cycle number become more sensitive with increasing stress level.

3. The proposed creep constitutive equations for the loading and unloading processes give good agreement with actual observations independent of the creep cycle number and of the stress level in the loading and unloading processes, respectively. In these cases, material constants are varied for the difference in creep cycle in the loading and unloading processes.

4. Although the features of cyclic creep behaviour mentioned above are obtained for the cellulose nitrate, it may be considered that the similar phenomena may appear in the cyclic behaviour for many polymers.

References

1. T. NISHITANI, *J. Mater. Sci.* **12** (1977) 1185.
2. T. NISHITANI and Y. DEGUCHI, *ibid.* **17** (1982) 779.
3. K. ONARAN and W. N. FINDLEY, *Trans. ASME J. Appl. Mech.* **38** (1971) 30.
4. A. COWKING, *J. Mater. Sci.* **10** (1975) 1751.
5. C. BAUWENS-CROWET and J. C. BAUWENS, *ibid.* **10** (1975) 1779.
6. Yu. N. RABOTNOV, "Creep Problems in Structural Member" (North-Holland, Amsterdam, 1969) p. 273.
7. Y. OHASHI, *Brit. J. Appl. Phys.* **16** (1965) 985.
8. T. NISHITANI and Y. KOIKE, *Strain* May (1981) 47.

Received 22 November 1991
and accepted 18 March 1992